EXPERIMENTAL INVESTIGATION OF OFFSHORE WAVE BUOY PERFORMANCE

Hamid Sarlak [1*], M.S. Seif [2] and M. Abbaspour [3]

1-M.Sc. Graduate, School of Mechanical Engineering, Sharif University of technology
2-Professor, School of Mechanical Engineering, Sharif University of Technology
3-Professor, School of Mechanical Engineering, Sharif University of Technology

Abstract

The important characteristic of sea waves is their high energy density, which is the highest among renewable energy sources. Having up to 2700 km. of shoreline, Iran has a great potential in construction of offshore wave buoys (hereafter called OWB). In this article a OWB model with the possibility of assembling different buoy configurations is introduced. The system is exposed to regular and irregular waves which are generated using wave maker in a 2D wave tank. Wave energy can be extracted from vertical oscillation of its floating buoy. The device is so designed as to operate in rotational (pitch) mode in addition to vertical (heave) motion.
Some experiments are also conducted to demonstrate system performance. Experimental results in different conditions are presented and the effect of different buoy configurations on the system efficiency is studied. Numerical simulations that obtain the hydrodynamic coefficients and dynamic response (the Response Amplitude Operator or simply RAO) of each buoy in waves validate test results that the buoy with highest transfer function obtained in simulations has highest efficiency in power extraction. It is finally shown that the horizontal buoy is the most efficient configuration among other constructed buoys for extracting wave energy. The non-dimensional groups are studied and the output power of a full scale OWB is obtained based on similarity laws.

Keywords: Offshore wave buoy, Hydrodynamic analysis, Model study

1. INTRODUCTION

The energy contained in marine environment can be extracted using Thermal, Wave, and current based devices. In ocean thermal energy converters (OTEC), the difference between water temperatures in different water depths change into useful energy. Wave and current energy devices, also, harvest the kinetic and potential energy of waves and currents to produce electrical energy.
Wave energy is created by wind, as a result of the atmosphere's redistribution of solar energy. The key characteristic of sea waves is their high energy density, which is the highest among renewable energy sources [1].

With having up to 2700 km. of shoreline in addition to big rivers, Iran has a great potential to develop marine energy power plants. The wave energy content often is measured in kW per meter of wave front. Figure 1 shows the wave power estimates around the world coasts [2].
Figure 1 shows that the average wave power near Chabahar in south-east coast of Iran is approximately 15 kW/m. Different wave energy converters have been developed in the world to use this source of energy.
Because of great potential in ocean waves, many devices have been developed for wave energy conversion purpose. One of the oldest yet efficient

*Corresponding Author: sarlak@alum.sharif.edu

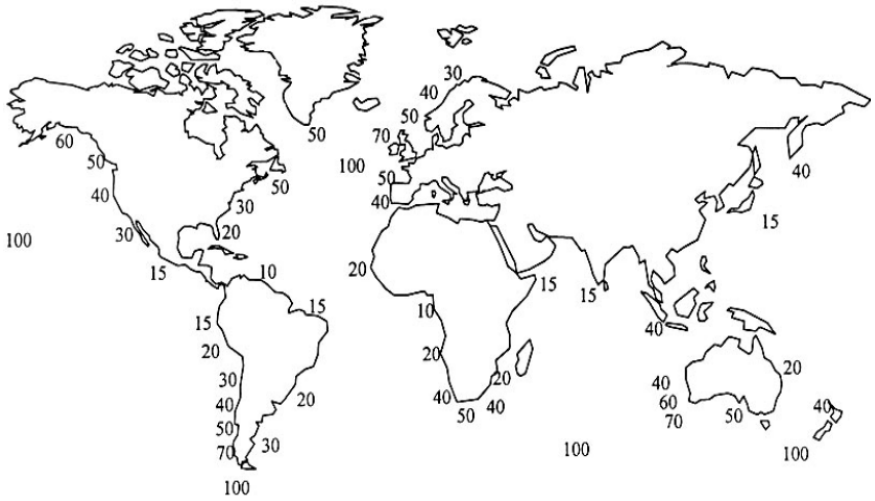

Fig. 1-Global mean wave power estimates in kW/m [2]

ways of ocean energy conversion is to utilize floating body motions in waves.

Girard [3] (late 18th century) was among the pioneers who discovered the energy contained in waves. He registered the first patent as a device which converts the wave power into mechanical energy. During 19th and 20th centuries some researchers studied and tested offshore wave energy power plants of different types; however the demand for renewable energy has dumped because of oil resources exploration during the 1st World War [4]. Major political and economical changes in the Middle East since 1970 such as the energy crisis (1973) as a result of Israel-Arabs war, and the Islamic revolution (1979) in Iran, urged the nations to change their energy policy [4]. Therefore, studies on renewable energy production systems re-started.

Falnes developed a configuration named REWEC that used the heave motion of a cylindrical floater relative to a surrounding outer cylinder to extract the wave energy [5]. Budal and Falnes proposed a latching control strategy that enhanced the power absorption of heaving OWB [6]. Larson and Falnes introduced a heaving buoy wave energy conversion with phase control and hydraulic power take-off that increase power capture by a factor of 2.8 or 4.3 in certain frequencies [7].

2. GOVERNING EQUATIONS

The form of energy contained in sea waves are investigated in this section. The total energy (E) is defined as the sum of potential and kinetic energies of waves per unit surface area. The power per unit wave length (P) is also defined as

$$E = \frac{1}{8}\rho g H^2 \quad [\frac{J}{m^2}]$$
$$P = E.C_g = \frac{1}{8}\frac{\rho g H^2 \lambda_n}{T} \qquad [\frac{W}{m}] \tag{1}$$

Where λ is wave length, H is wave height, T is wave period, C_g is group velocity and g is gravitational acceleration. Figure 2 shows a 2D sketch of wave tank as well as a free body schematic of OWB. A floating buoy oscillates in vertical (Heave) mode on wave surface due to the excitation from

incoming waves. Thus the equations of motion for the oscillating buoy can be written as

$$\sum F_{external} = m_{buoy}\,\ddot{z} \qquad (2)$$

Where the first term is the sum of external forces exerted on the buoy. m_{buoy} is buoy mass, and $\ddot{z}$ is vertical acceleration.

As shown in Figure 2, the external force contains gravity force ($F_w = -kgz$), generator force ($F_{gen} = -\gamma\dot{z}$) (where kg and γ are defined as restoring and generator damping coefficients, and z and $\dot{z}$ are buoy position and velocities in vertical direction), and the wave excitation force which includes three hydrodynamic components ($F_{wav} = F_e + F_r + F_h$).

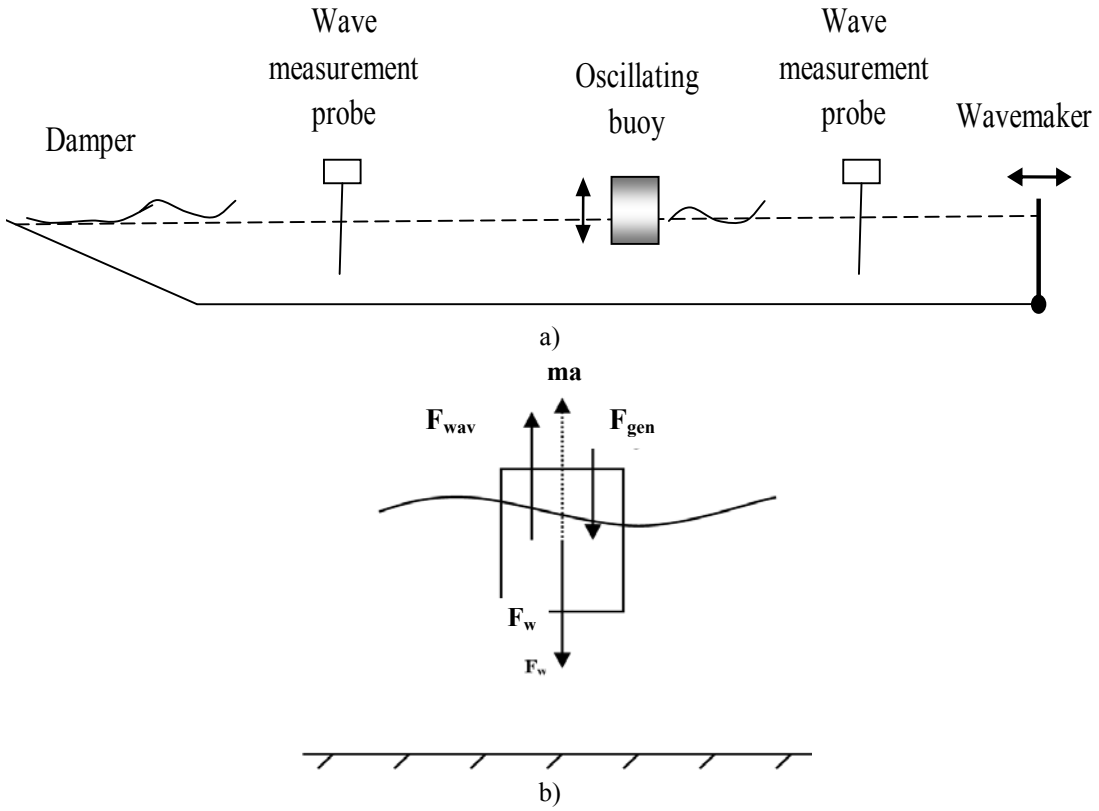

Fig. 2 a) Schematic view of the problem b) forces acting on floating buoy

Where F_r is the force due to radiation of waves from oscillating buoy in calm water, F_e is the exciting force due to scattering of incident wave approaching a body fixed in water, and F_h is the buoyancy (stiffness) force exerted on the buoy. Solution of equation (2) results in the following relation:

$$(m+A_{33})\ddot{z} + B_{33}\dot{z} + C_{33}z = F_{extemd}(t) \qquad (3)$$

In this equation A_{33}, B_{33} and C_{33} represent added mass, damping and restoring coefficients, respectively.
Finally, heave RAO, which is the ratio between buoy heaving motion and wave amplitudes and has an important role in OWB dynamics, can be driven as [7]

$$RAO = \frac{F}{-\omega^2(M + A_{33}) + i\,\omega B_{33} + C_{33}} \quad (4)$$

A common method for estimating hydrodynamic coefficients to obtain buoy response is Strip Theory. This method, originally developed in the 1970s (Salvesen et al. 1970) is useful for many applications in marine dynamics [8].
In this paper added mass and damping coefficients are estimated using strip theory which is explained in next part of this section.
After finding the above coefficients, time domain solution of buoy motion can be obtained using ODE solving techniques like Runge-Kutta method.

2.1. HYDRODYNAMIC SIMULATION

The simulations of freely floating buoys are done using Seakeeper® software. This package simulates behavior of dynamical systems in real irregular seas as well as regular laboratory wave conditions. The characteristics of different buoys are presented in Table 1.

Table1. buoy configurations for simulation and test

Buoy shape	L (or H) [m]	R [m]	draft	VCG
Vertical Cylinder	0.27	0.2	0.1	0.1
Horizontal Cylinder	0.9	0.2	0.1	0.1
Wedge (box)	0.4	-	0.1	0.1
Hemisphere	-	0.4	0.1	0.1

Strip theory is a frequency-domain method which is based on potential flow theory. The main advantage of solving problems in frequency domain is the considerable time-saving in computations [8].
In strip theory, the buoy is split into a number of transverse sections. Each of these sections is then treated as a two-dimensional section in order to compute its hydrodynamic characteristics. The coefficients for the sections are then integrated along the length of the hull to obtain the global coefficients of the equations of motion of the whole vessel. Finally the coupled equations of motion are solved [8]. Further information about strip theory and dynamics of floating particles can be found in [9].
Figure 3 represents added mass, damping and restoring coefficients versus frequency for different buoys.
It is shown in figure that restoring moment has a nearly constant behavior in all frequencies; however, damping and added mass coefficients strongly depend on wave frequency.
Figure 4 illustrates buoys RAOs i.e. the ratio of buoy motion to wave elevation. TF can be used to calculate the floating body response in a number of wave frequencies.
As shown in Figure 4, the value of TF is approximately 1 for frequencies up to 1 Hz which means that the buoy response is the same as the wave amplitude. However, this response tends to become zero as the frequency of oscillation increases and for frequencies greater than 2 Hz, almost all of the buoy's RAOs tend to zero and the buoys do not respond to wave excitation.

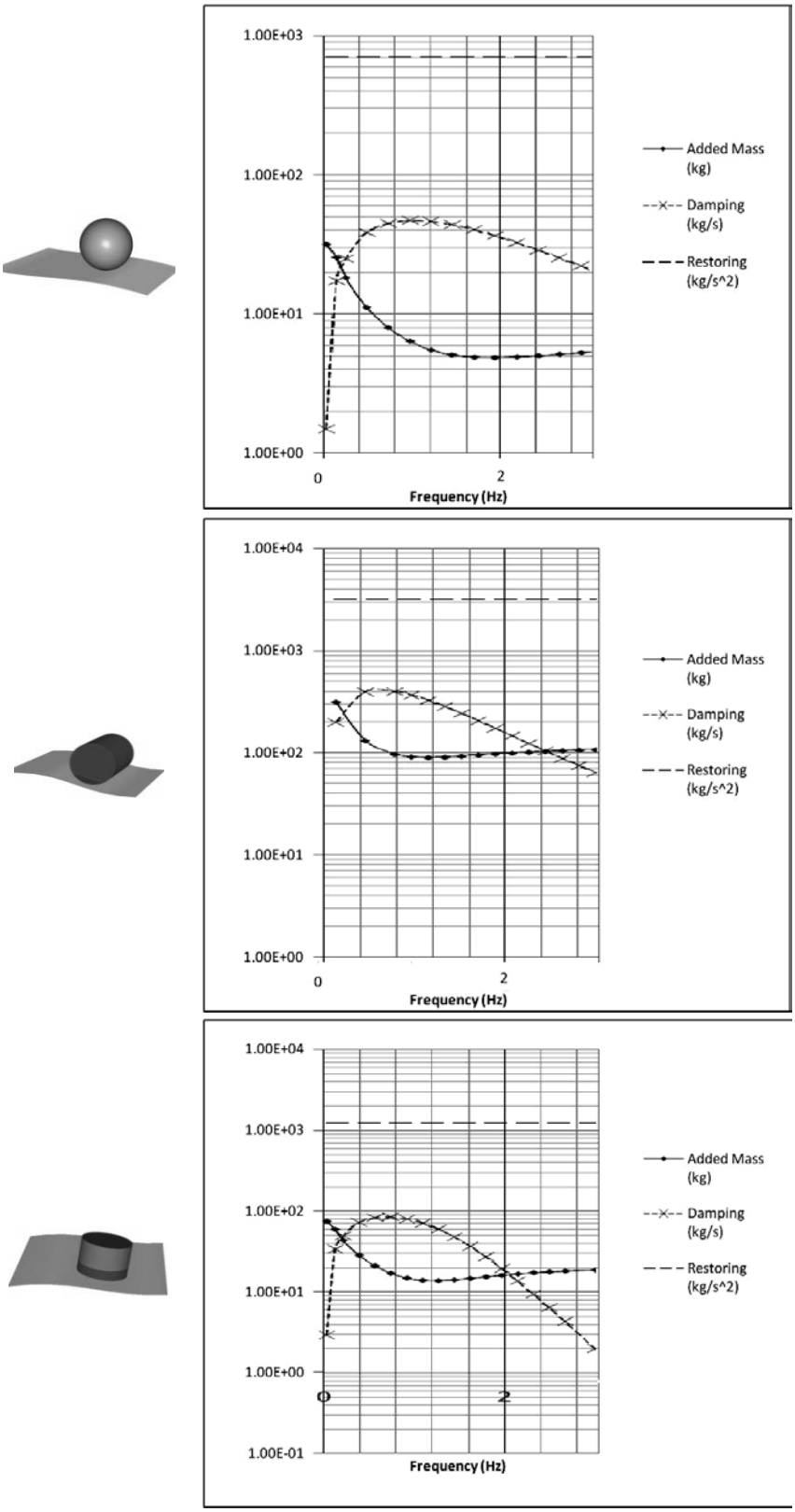

Fig. 3- buoys hydrodynamic coefficients

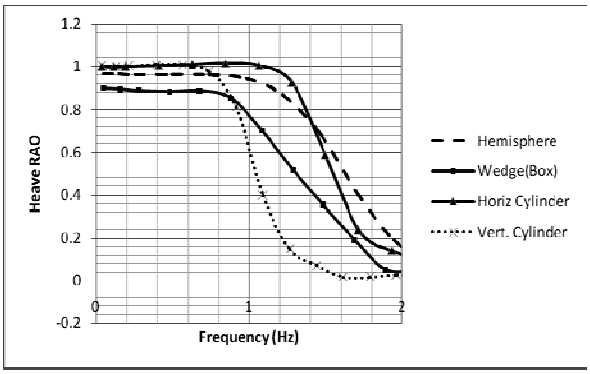

Fig. 4- RAOs for different buoys

2.2. SCALE EFFECTS

In order to establish similarity law to design the real OWB based on model test results, The Froude (Fr), as well as Strouhal (St) numbers and wave steepness should be the same between the model and real prototype. Thus, we have

$$(F_r)_m = (F_r)_p \rightarrow \frac{v_m}{\sqrt{gL_m}} = \frac{v_p}{\sqrt{gL_p}}$$

$$\frac{v_m}{v_p} = \frac{\sqrt{gL_m}}{\sqrt{gL_p}} = \sqrt{\lambda}$$

$$St_m = St_p \rightarrow \frac{f_m L_m}{V_m} = \frac{f_p L_p}{V_p} \rightarrow \frac{L_m}{T_m v_m} = \frac{L_p}{T_p v_p} \quad (5)$$

$$\frac{T_m}{T_p} = \frac{L_m}{L_p}\left(\frac{v_p}{v_m}\right) = \sqrt{\lambda}$$

$$\frac{H_m}{l_m} = \frac{H_p}{l_p} \quad (H \text{ and } l : \text{wave height and length})$$

Where *m* and *p* subscripts stand for model and prototype, v, L, T are characteristic velocity, length and time and λ indicates scale factor. So the relation between the model and real prototype becomes as shown in Table 2.

Table2. Similarity law for OWB design [7]

Parameter	Model	Prototype
length	1	λ
speed	1	$\lambda^{0.5}$
force	1	λ^{3}
Power	1	$\lambda^{3.5}$

In other words, to obtain similarity, the wave length in which the real prototype is to be tested should be λ times the wave length produced in laboratory and in this condition the absorbed power from real prototype is expected to be $\lambda^{3.5}$ times the power obtained in laboratory measurements.

3. MODEL CONSTRUCTION AND INSTALLATION

In this section the construction and installation of OWB in the wave tank are presented. First, the different buoys are constructed using special water tight sponge two samples of which are shown in Figure 5. Different buoys include horizontal cylinder with 0.4 m diameter and 0.9 m length, vertical cylinder with 0.4 m diameter and 0.27 m height, wedge with 0.2 m and 0.4 m lower and upper bases respectively and 0.27 m height and hemisphere with 0.4 m diameter.

The buoy assemblage is constrained to the main frame (and the frame is fixed to the tank) using a strut of length 50cm that slides through an linear type guide (bearing). As shown in Figure 5, mechanical system that consist of gearbox (ratio: 1:6) and a rack-pinion mechanism as well as a generator located at the end of strut and convert the linear motion of buoy to rotational motion.

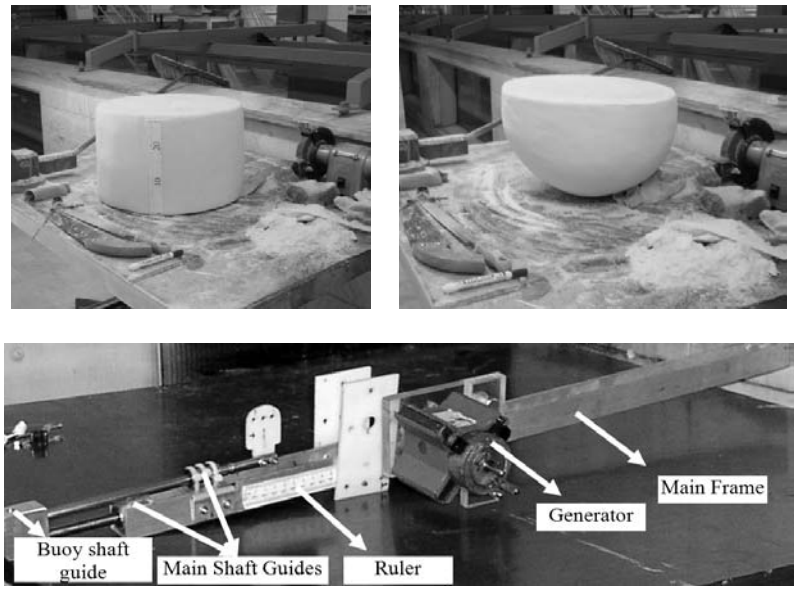

Fig. 5- OWB construction process in Marine Engineering Laboratory

A complete configuration of device is shown in Figure 6-a. Figure 6-b shows the installed model of OWB with horizontal buoy configuration in wave tank. The time history of the buoy motion can be measured by an accelerometer which is installed on the top of the buoy. The system extracts the maximum energy from waves in case that the buoy natural frequency and wave frequency become close to each other. An important way to achieve this, is applying control mechanisms such as latching control which is explained in detailed in [6].

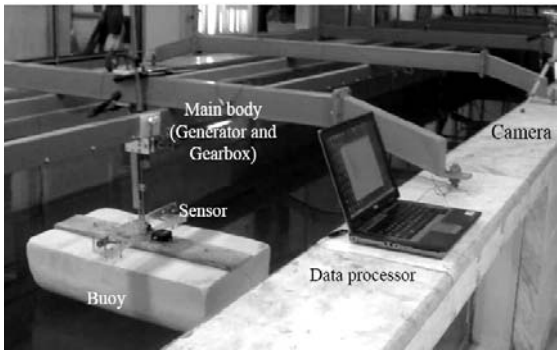

Fig. 6a- Completed OWB with measurement devices

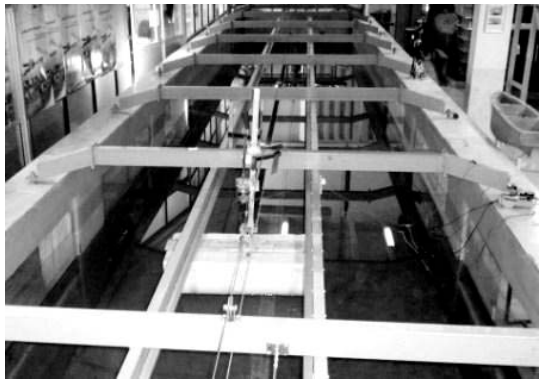

Fig. 6b- installation of OWB in wave tank

4.EXPERIMENTAL MEASUREMENTS

4.1. TEST SETUP

The experiments were carried out in Marine Engineering Laboratory at School of Mechanical Engineering, Sharif University of Technology. The channel is 25 m long, 1.7 m wide and 1.3 m high. A paddle-type wave generator is developed which can generate unidirectional waves with a maximum height of 0.12 m and 0.5–1.5 s periods. The height of the waves is measured at any point in the channel using image-processing. Figures 7 and 8 show the paddle-type wave maker developed in the wave tank of Marine Engineering

Laboratory and a sample generated wave. Partly captive tests in which the model is free to heave (vertical motion) and restrained in other modes of motion is carried out in the tank.

3.2. RESULTS

For the measurement of output power, two digital multimeters are used; one for voltage measurement and the other for current measurement. Finally, the output power is obtained using equation 6.

$$P_{extracted} = V \times I \qquad [W] \qquad (6)$$

Where V (voltage) is measured in volts and I (current) in amperes.
Buoy particulars are identical to those given in Table 1 for hydrodynamic simulation. In each test the device is exposed to waves of 0.05 m average height and 1 s period. Figure 9 shows the assembly with horizontal buoy.

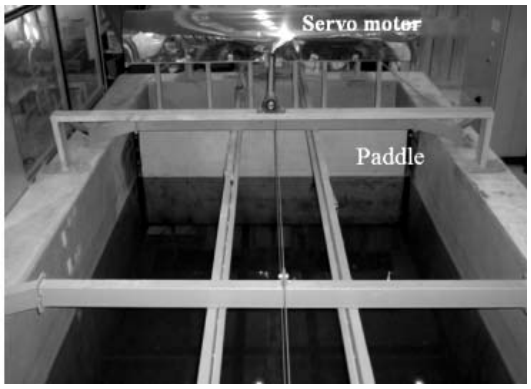

Fig. 7- Wave flume and developed wave maker system

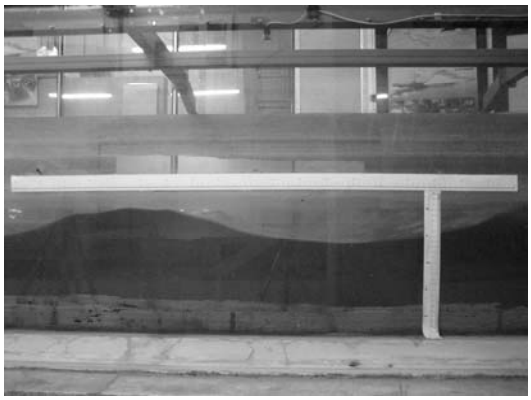

Fig. 8- Sample of wave generated in Marine Engineering Laboratory wave tank

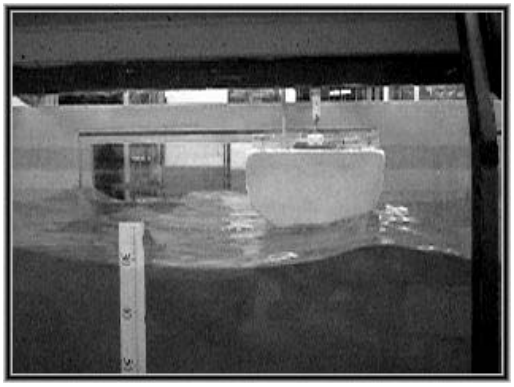

Fig. 9- horizontal Cylinder OWB set up

Figure 10-a shows that measured current ranges between 0.0 and 0.5 A, Figure 10-b. shows that measured voltage ranges between 0.1 and 1.7 Volts and 10-c shows that their cumulative product i.e. output power ranges between 0.05 and 0.65 W with an average of 135 mW in 50s test sample.

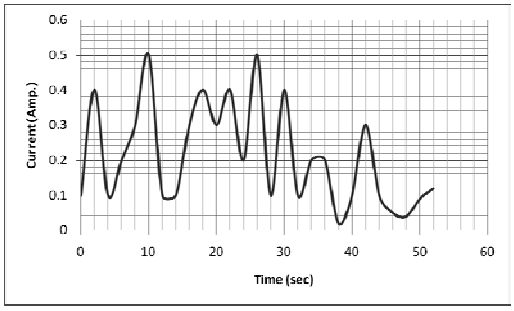

Fig. 10a- horizontal Cylinder type OWB measured current

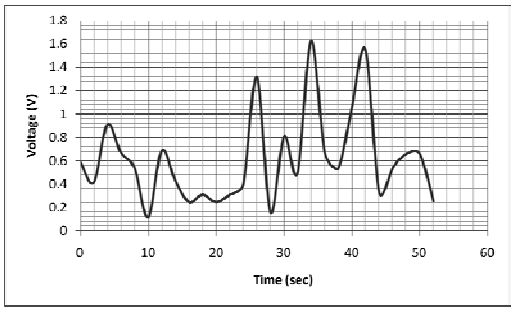

Fig. 10b- horizontal Cylinder type OWB measured voltage

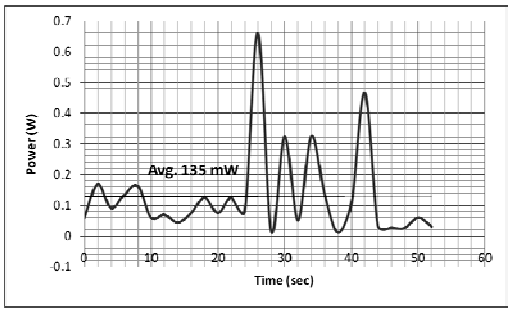

Fig. 10c- horizontal Cylinder type OWB measured power

Figure 11 shows the assembly with vertical buoy.

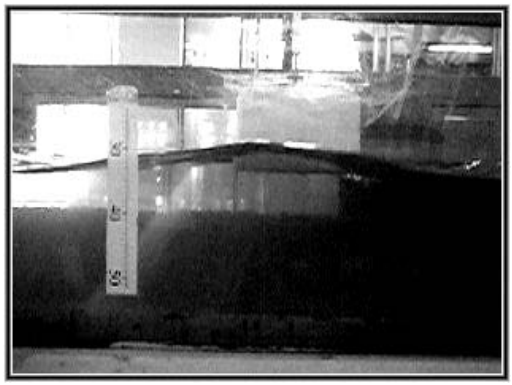

Fig. 11- Vertical Cylinder buoy configuration of OWB

Figure 12-a shows that measured current ranges irregularly between 0.0 and 0.62 A, the measured voltage as shown in Figure 10-b. ranges between 0.0 and 0.7 Volts and 10-c shows the cumulative product i.e. output power which is fluctuating between 0.0 and 0.14 mW with an average of 32 mW in 50s test sample.

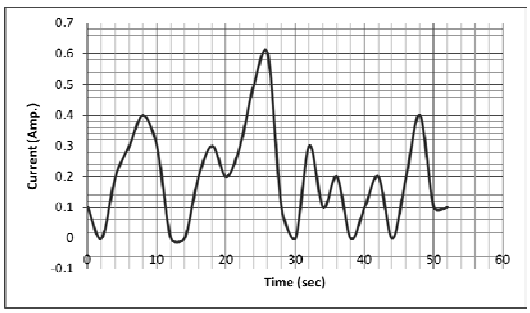

Fig. 12a- Vertical Cylinder type OWB measured current

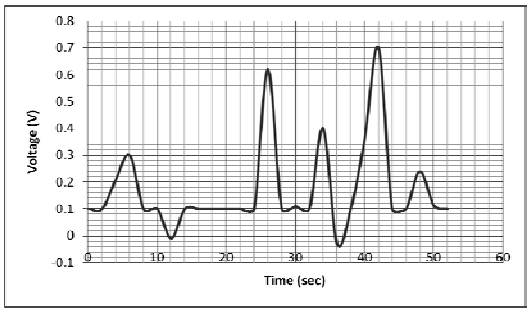

Fig. 12b- Vertical Cylinder type OWB measured voltage

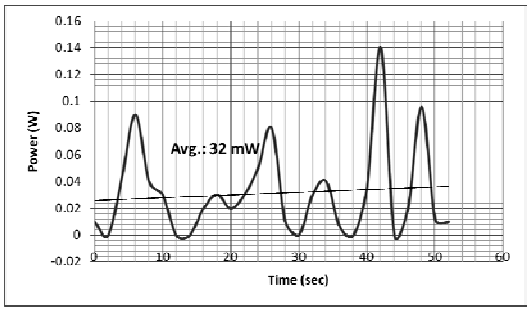

Fig. 12c- Vertical Cylinder type OWB measured power

Figure 13 shows the assembly with wedge buoy.

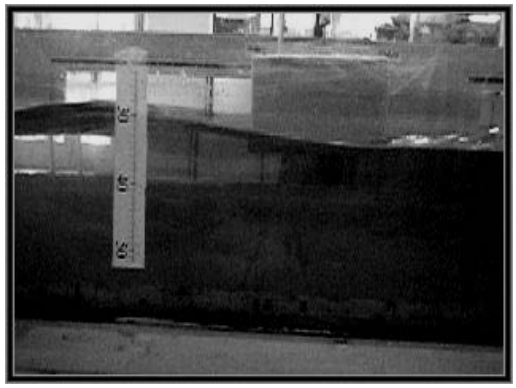

Fig. 13- Wedge shape buoy configuration of OWB

Figures 14-a through 14-c show that measured current ranges between 0.0 and 0.32 A, measured voltage ranges between 0.0 and 0.6 Volts and that their cumulative product i.e. output power ranges between 0.0 and 0.09 W with an average of 14 mW in 50s test sample.

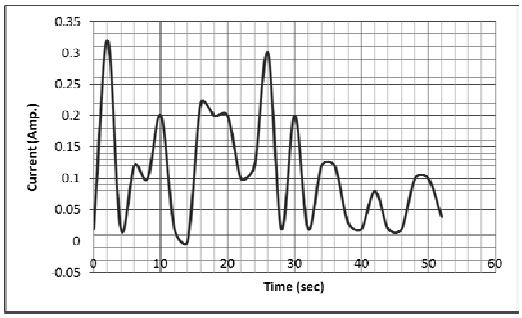

Fig. 14a-Wedge type OWB measured current

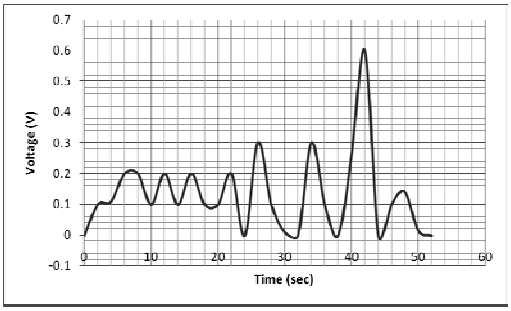

Fig. 14b-Wedge type OWB measured voltage

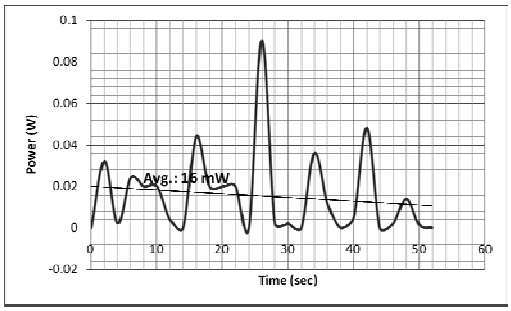

Fig. 14c- Wedge type OWB measured power (W)

Figure 15 shows the assembly with hemisphere buoy.

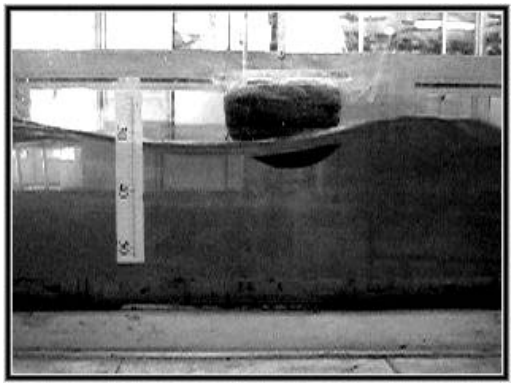

Fig. 15- Hemisphere buoy configuration of OWB

Figures 16-a through 16-c show that measured current ranges between 0.0 and 0.45 A, measured voltage between 0.0 and 0.62 Volts, and the output power between 0.0 and 0.08 W with an average of 21 mW in 50s test sample.

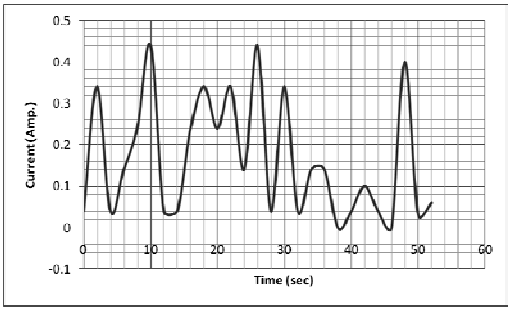

Fig. 16a- Hemisphere type OWB measured current

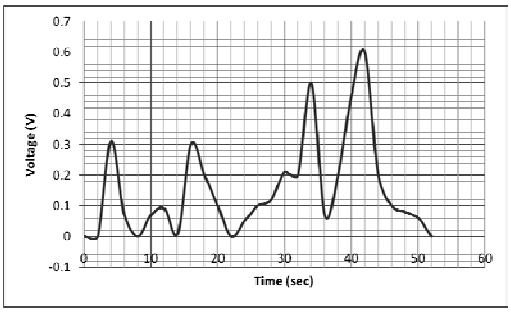

Fig. 16b- Hemisphere type OWB measured voltage

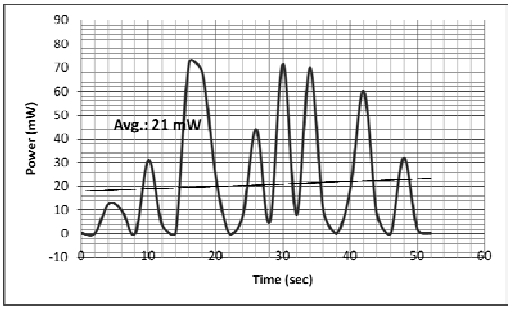

Fig. 16c- Hemisphere type OWB measured power

So the output power is measured 135, 32, 16, and 21 mW for horizontal cylinder, vertical cylinder, wedge, and hemisphere buoys respectively. The available power is calculated using equation 1; and the efficiency of system is defined as

$$Eff. = \frac{P_{extracted}}{P_{available}} = \frac{V.I \quad (W)}{\left(\frac{\rho g H^2 \lambda b_{buoy}}{8T}\right) \quad (W)} \quad (7)$$

Figure 17 shows the comparison of efficiencies obtained for different buoy shapes. According to the figure, the efficiency of horizontal buoy, hemisphere, vertical cylinder and wedge type wave energy power plants are 10%, 7%, 5.2% and 4.2%, respectively.

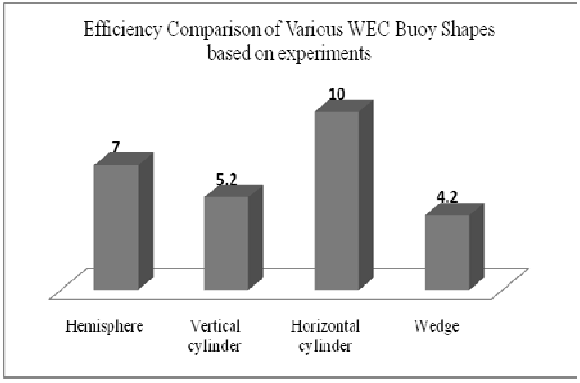

Fig. 17- performance of OWB

5. CONCLUSION

In this paper, the performance of a OWB model was studied using mathematical simulation and laboratory model test. First, the performance of different buoy shapes were compared using strip theory simulations. It was shown that heave RAO is about 1 for frequencies below 1 Hz and falls down to zero as frequency approaches higher values. Then a wave energy power plant was developed and tested with four different buoys with which the simulations were carried out. The device were tested against different waves in wave tank and output power of each case were measured meanwhile. The efficiency was defined as the ratio of extracted power to the available power and the efficiencies of different buoys were calculated.

As shown in the research, the horizontal buoy wave energy power plant is considered the most effective among other configurations. According to similarity laws stated in the previous section, the output capacity of a 100th scale real size OWBs will be 1350, 320, 160 and 210 kW for horizontal cylinder, vertical cylinder, wedge, and hemisphere-buoy power plants, respectively. Such work has been neither indexed in national databases yet nor such usage of mechanical power take off mechanism (gearbox, rotary generator) does seem to be appeared in other researches papers i.e. most researches (e.g. ref. [7]) are carried out using a set of linear generators without power transmission devices.

8. REFERENCES

1-Clement A, McCullen P, Falcao A, Fiorentino F, Gardner F, Hammarlund K, (2002), "Wave energy in Europe: current status and perspectives", Renewable Sustainable Energy Report.

2-J. Cruz, (2008), *Ocean wave energy, current status and future perspective*, 1st ed., Springer Verlag.

3-Patent of invention for 15 years, employ the sea waves as motors, (1799), Paris, France. (in French).

4-Encyclopedia of Encarta®, (2008), ed., Microsoft® Corporation.

5-Falnes, J., McIver, P., (1985), "Surface wave interactions with systems of oscillating bodies and pressure distributions". Journal of Applied Ocean Research 7 (4), 225–234

6-K. Budal, J. Falnes, (1980), "Interacting point absorbers with controlled motion Power from Sea Waves", Academic Press, London, pp. 381–399.

7-G. P. Gore, (2007), "Scaled modeling and Simulation of Ocean Wave Linear Generator Buoy Systems", PhD Thesis, Oregon University.

8-Seakeeper® 11 theory manual, (2005), Formation design system.

9-J. N. Newman, (1999), *Marine Hydrodynamics*, MIT Press, 9th Ed.